Journal of Applied Fluid Mechanics, Vol. 18, No. 10, pp. 2453-2464, 2025.
Available online at www.jafmonline.net, ISSN 1735-3572, EISSN 1735-3645.
https://doi.org/10.47176/jafm.18.10.3384

Performance and Hydrodynamics of a Bent Riser Airlift Pump

S. Z. Kassab[1], A. A. Abdelrazek[1] and E. R. Lotfy[1,2†]

[1] *Mechanical Engineering Department, Faculty of Engineering, Alexandria University, 21544 Alexandria, Egypt*
[2] *Department of Energy Resources Engineering, Egypt-Japan University of Science and Technology, 21934 Alexandria, Egypt*

†*Corresponding Author Email: eslam.reda@alexu.edu.eg*

ABSTRACT

Airlift pumps are commonly employed in oil and gas operations, utilising the upward motion of a gas-liquid mixture driven by buoyancy and density contrasts. While numerous investigations have focused on their behaviour in vertically aligned straight pipes, the influence of pipe curvature—particularly relevant in directional drilling—has not been extensively explored. This work provides a comprehensive experimental assessment of how bends affect the hydraulic performance and flow dynamics of airlift systems. Five bent riser configurations were tested and compared with a conventional straight riser, with emphasis on variations in bend height and horizontal spacing. The findings reveal that pump efficiency diminishes as the horizontal distance between bends increases or when bends are positioned higher along the riser. Specifically, a 15% reduction in water flow rate occurred when the bend's horizontal span reached twice the pipe diameter. Additionally, a 6% drop was observed when a bend was introduced at three-quarters of the riser height. The minimum air flow rate required to initiate water lifting also increased when bends were placed above the submergence level. Visual flow analysis further identified cyclic flow behaviour within the bent sections. These insights offer practical guidance for enhancing airlift pump designs in non-vertical geometries, addressing notable gaps in two-phase flow system optimisation.

Article History

Received January 17, 2025
Revised April 24, 2025
Accepted May 4, 2025
Available online August 5, 2025

Keywords:

Efficiency
Experimental
Flow patterns
Flow visualisation
Gas lift pump
Geometry
Hydrodynamics

1. INTRODUCTION

Airlift pumps operate without mechanical components, relying instead on the injection of compressed air to transport liquids and suspended solids. Their simplicity and lack of moving parts make them attractive for a wide range of applications, from waste management and aquaculture water circulation to the oil and gas sector and the handling of hazardous or abrasive materials (cho et al., 2009; Hu et al., 2012; Qiang et al., 2018; Shallouf et al., 2019; Enany & Drebenshtedt, 2024; Kumar et al., 2024). This broad applicability has spurred sustained research interest in enhancing their operational efficiency.

In oil production, when natural reservoir pressure declines below the level required for economically viable extraction, artificial lift techniques become necessary. These include methods such as sucker rod systems, subsurface hydraulic or jet pumps, electric submersible pumps, and gas lift systems. Gas lift, which utilises high-pressure gas injected downhole to lighten the hydrocarbon column and restore flow, is particularly beneficial where gas is readily available (Okon & Ndubuka, 2023).

Fan et al. (2013) conducted both theoretical and experimental studies on the use of airlift pumps for artificial upwelling, showing that performance depends heavily on pipe geometry, air injection strategy, and the stratification of water density. Their later work (Fan et al. 2020) further explored how such systems contribute to carbon removal and thermal and nutrient distribution in coastal waters.

Because airlift operation involves gas-liquid mixtures, understanding two-phase flow behaviour is essential. The system can display various flow regimes: bubbly flow dominates at low gas injection rates, while annular flow—linked to settled liquid throughput—emerges at high rates. Optimal performance typically falls within the slug and churn flow regimes, where the pump gives the maximum liquid productivity relative to input gas power (Kassab et al., 2022).

Previous investigations have also examined the effects of non-standard riser geometries. For example, Hanafizadeh et al. (2010) numerically analysed tapered risers and found increased water flow rates with larger divergence angles. Kassab et al. (2023) recently performed

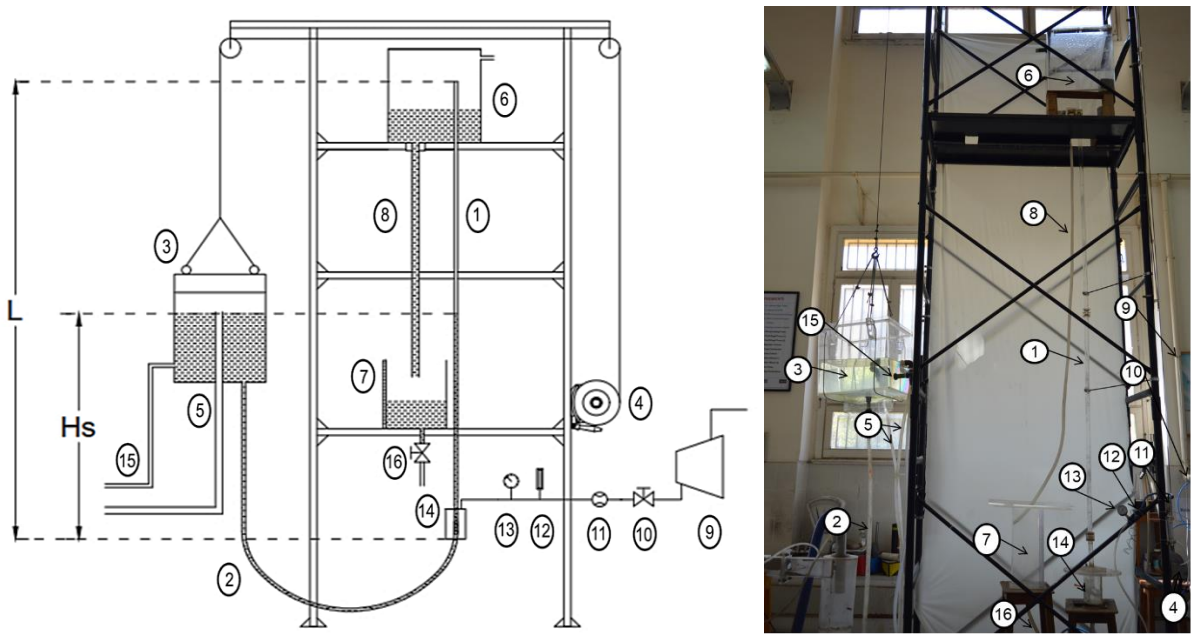

1	Riser pipe	5	Overflow pipe	9	Compressor	13	Pressure gauge
2	Down-comer	6	Overhead tank	10	Pressure regulator	14	Air injector
3	Supply tank	7	Measuring tank	11	Air flow meter	15	Water supply pipe
4	Winch crane	8	Drain	12	Thermometer	16	Drain valve

Fig. 1 Schematic diagram of the experimental set up

experimental studies on the impacts of sudden expansions and contractions in riser diameter, confirming their influence on throughput and efficiency. Additionally, Fujimoto et al. (2004) introduced S-shaped bends into the riser to assess three-phase flow dynamics, concluding that such bends reduce solid transport and overall performance—especially when located above the air injection point.

Despite a strong research focus on straight, vertical risers, practical installations frequently require bent or irregular geometries. This is especially true in directional drilling, where deviations from verticality are common due to structural constraints or operational needs (Arabjamaloei et al., 2011; Elbanna, 2016). These include drilling from a single platform to reach multiple targets, bypassing inaccessible or hazardous surface zones, or increasing reservoir contact to enhance recovery.

Given that any deviation from a vertical riser typically results in performance degradation, it is crucial to examine how such configurations affect airlift operation. However, research addressing the hydrodynamics and efficiency of airlift pumps with bent risers is limited. The current study addresses this gap by experimentally analysing how bends—at various locations and with different geometric spans—impact performance. Specifically, it quantifies the extent of productivity loss and examines the flow characteristics within bent configurations, providing novel insights for optimising non-vertical airlift pump systems.

This research builds upon over four decades of foundational work carried out by the fluid mechanics group at the Mechanical Engineering Department, Alexandria University, as detailed in (Kassab et al., 2022).

2. EXPERIMENTAL SETUP

Figure 1 shows a schematic diagram of the experimental system developed to evaluate the performance of airlift pumps under varying geometric configurations. The core of the system is a transparent vertical riser pipe (1), made from acrylic, with an internal diameter of 24 mm and a total height of 4 metres. Water is supplied to the riser via a flexible inlet hose (2) connected to a storage tank (3), which measures 70 × 70 × 80 cm. A manual winch crane (4) allows vertical adjustment of the tank, thereby modifying the static head Hs and the submergence ratio. Excess water from the tank is discharged through an overflow pipe (5).

The riser directs the discharged water to an upper collection tank (6) with dimensions of 70 × 100 × 100 cm, open to atmospheric pressure. This tank is further linked to a calibrated measuring container (7), sized 15 × 20 × 50 cm, through a drain hose (8), allowing accurate measurement of the delivered flow rate.

Air required for pump operation is supplied by a compressor (9), and is conditioned by passing through a drying unit, filtration components, and a pressure regulator (10). Airflow is measured using a vertically mounted rotameter (11), with a thermometer (12) and a calibrated pressure gauge (13) placed along the line for monitoring. Air is introduced into the riser through a specially designed injection jacket (14) that distributes the air evenly via a matrix of 56 holes (7 rows × 8 columns), each 3 mm in diameter, based on Kassab et al. (2009)'s configuration.

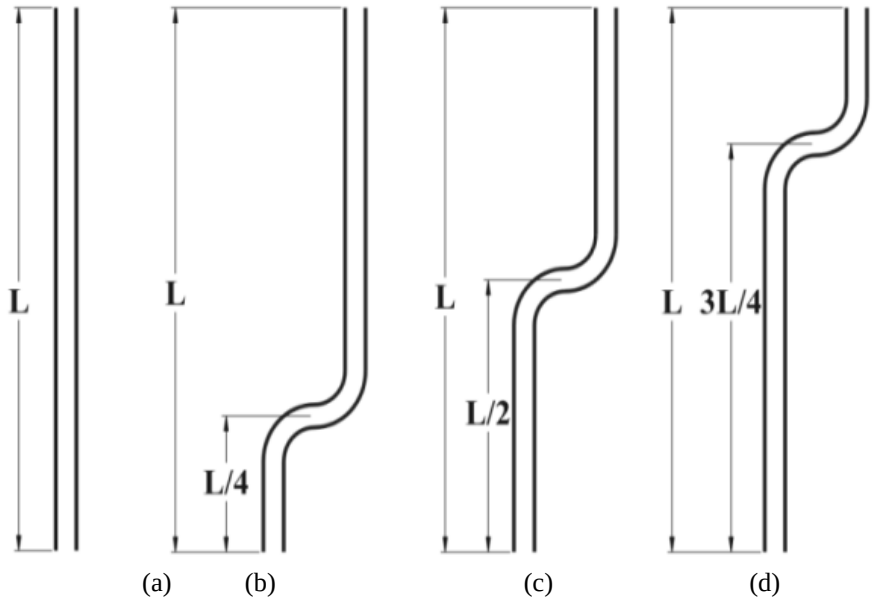

Fig. 2 Schematic of the examined bend mounting elevations

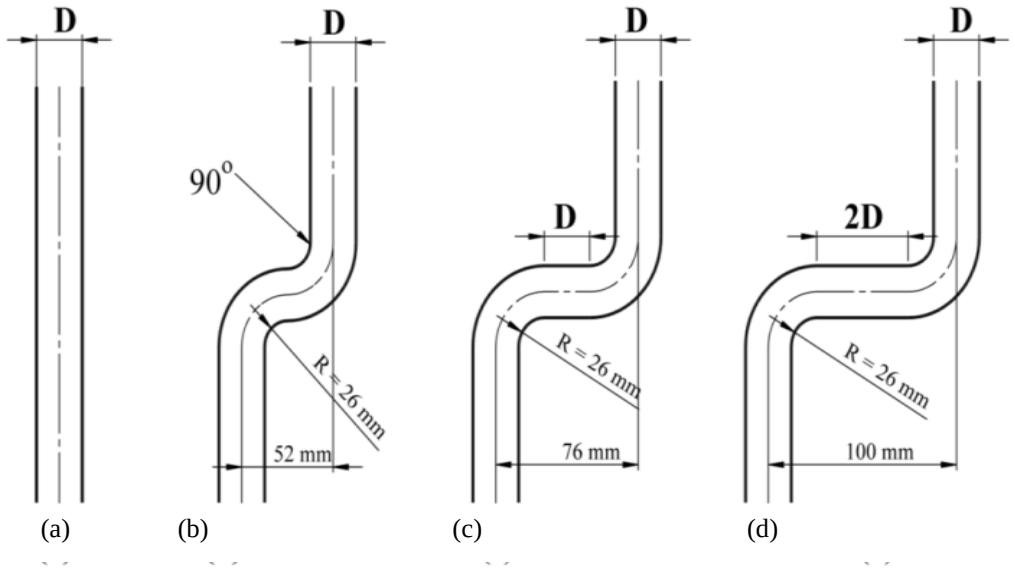

Fig. 3 Schematic of the examined bend span lengths

To facilitate flow pattern observation, both the riser and its bends were constructed from transparent material. A high-speed camera (240 frames per second) was positioned to record the flow behaviour, particularly around the bend region. A dark background and consistent lighting were used to enhance image clarity due to the fast shutter speed.

The experiments compared a straight riser with bent risers containing two 90-degree elbows. Five configurations were tested: three variations in vertical bend placement (at L/4, L/2, and 3L/4) and three different horizontal spans between elbows (0, D, and 2D), as illustrated in Figs. 2 and 3. Vertical location effects were studied using a zero-span configuration, while span variations were assessed at mid-height of the riser.

Across all configurations, the air mass flow rate was adjusted between 0.4 and 17 kg/s. The submergence ratio, defined as Hs/L, was fixed at 0.4 to match previously validated studies such as Kassab et al. (2009). While higher submergence ratios (up to 0.8) are commonly used in gas-lift operations in oilfields (Samaras & Margaris, 2005), this value was chosen to ensure comparability with existing benchmark data. Additional studies exploring high submergence conditions can be found in Kim et al. (2014) and Tighzert et al. (2013).

All measuring instruments were carefully calibrated using appropriate methods. Furthermore, uncertainty analysis was carried out based on the multivariate Taylor Series expansion, with the resulting uncertainty estimates summarised in Table 1.

Table 1 Measuring methods and estimated uncertainties

Quantity	Measuring method	Uncertainty (%)
Air flow rate	Air flow meter	3
Water flow rate	Recording the time to collect a volume of water	1.25
Temperature	Thermometer	1.17
Pressure	Pressure gage	2.5

3. RESULTS AND DISCUSSION

Figures 4 and 5 summarise the performance data for the airlift pump operating with a vertically straight riser pipe, as illustrated in Figs. 2a and 3a. These results serve as the baseline for evaluating the influence of pipe bends on the pump's performance.

Figure 4 provides visual documentation of the two-phase flow regimes that develop within the straight riser under varying air injection rates. At low gas flow rates ($\dot{m}_{air}$ < 0.8 kg/h), the flow is dominated by dispersed bubbles—known as the bubbly flow regime (Fig. 4a). Here, buoyant forces cause the bubbles to rise steadily, while turbulent mixing and surface tension suppress bubble merging. As the air injection rate increases to the range 0.8 < $\dot{m}$air < 1.8 kg/h, the gas volume fraction rises, intensifying bubble interactions. This results in the formation of larger gas pockets that span the riser's cross-section, transitioning the system into the slug flow regime (Figs. 4b and 4c), characterised by Taylor bubbles. The emergence of this regime is primarily due to enhanced gas inertia overcoming the resistance of surface tension and turbulence.

When the gas flow continues to rise (1.8 < $\dot{m}$air < 10.3 kg/h), the slug structures begin to disintegrate under the influence of vigorous turbulence, leading to a more chaotic and unstable pattern identified as churn flow (Figs. 4d and 4e). This regime lacks the regular bubble structure of slug flow and is marked by oscillating motions of both phases. At even higher flow rates ($\dot{m}$air > 10.3 kg/h), the system transitions into annular flow (Figs. 4f and 4g), where the gas forms a central core and the liquid is sheared into a thin film along the pipe walls. In this condition, entrained droplets may also appear within the core stream, a sub-pattern known as mist flow. The observed transitions between these flow patterns are consistent with experimental findings reported by Bukhari et al. (2024) and Doucette et al. (2024).

Figure 5 illustrates the relationship between water output and air mass flow rate for the straight riser configuration. The data show excellent alignment with the well-established experimental results of Kassab et al. (2009), providing strong validation for the current experimental methodology and reinforcing the reliability of the obtained measurements.

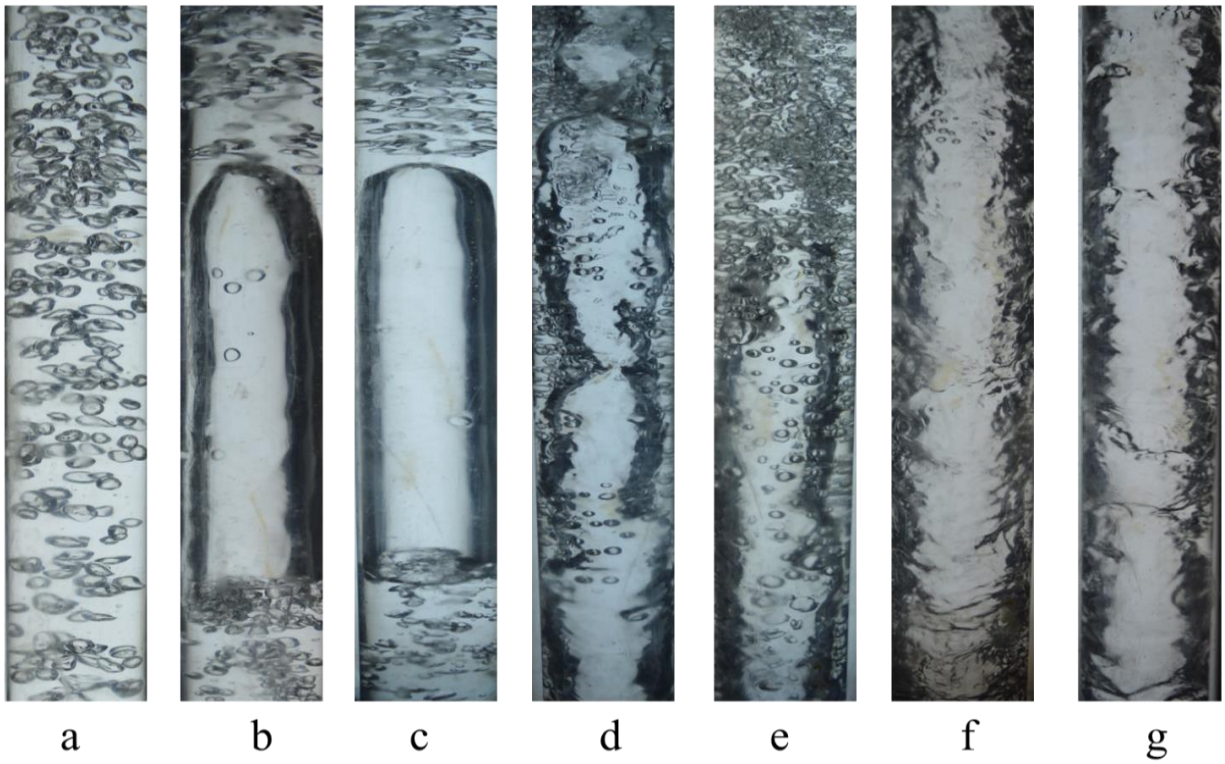

Fig. 4 Visualization of the various flow patterns present in the straight riser airlift pump: (a) bubbly flow, (b and c) slug flow, (d and e) slug—churn flow, (f and g) annular flow

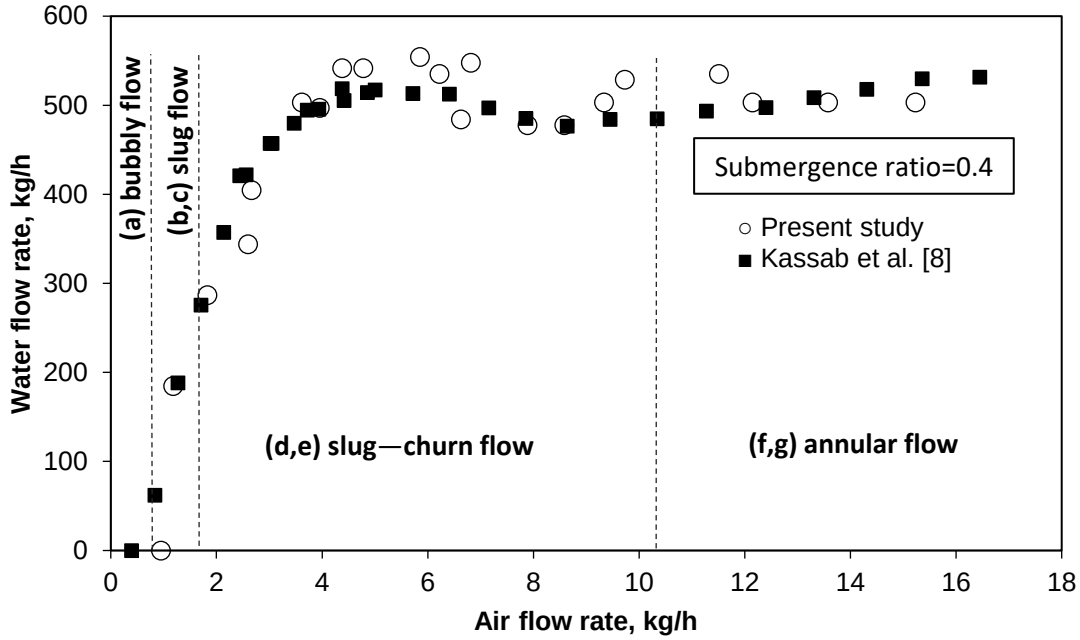

Fig. 5 Comparison between the results of the present study and Kassab et al. (2009) results. The flow regimes (a) through (g) are demonstrated in Fig. 4

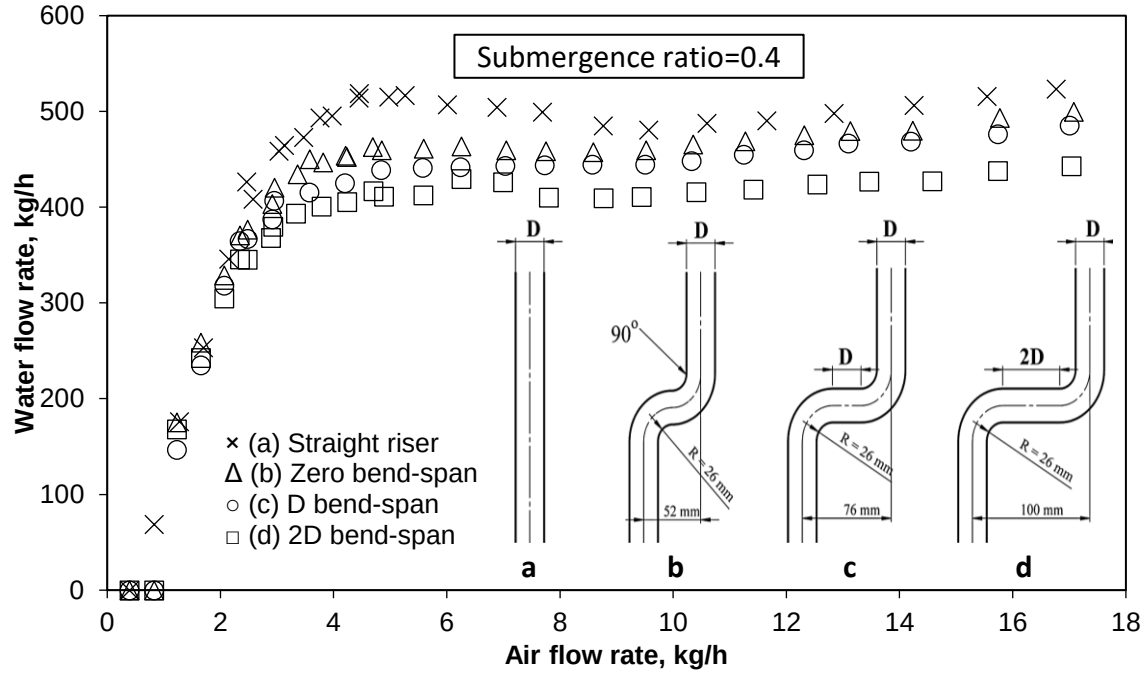

Fig. 6 Variation of water productivity with air mass flow rate for different bend-span lengths

3.1 Effect of Bend-Span Length

To examine how the horizontal spacing between bends affects pump performance, three riser configurations with span lengths of 0, D, and 2D were tested experimentally. Figures 6 and 7 present the corresponding trends in water flow rate and pump efficiency as functions of the air mass flow rate.

The airlift pump's efficiency is evaluated using the expression introduced by Nicklin (1963):

$$\eta = \frac{\rho_w \, g \, Q_w \, (L - H_s)}{P_{in} \, Q_{air} \, \ln \frac{P_{in}}{P_a}}, \tag{1}$$

where:

- ρ_w is the water density (kg/m^3),
- g is gravitational acceleration (m/s^2),
- Q_w and Q_{air} are the volumetric flow rates of water and air (m^3/s), respectively,

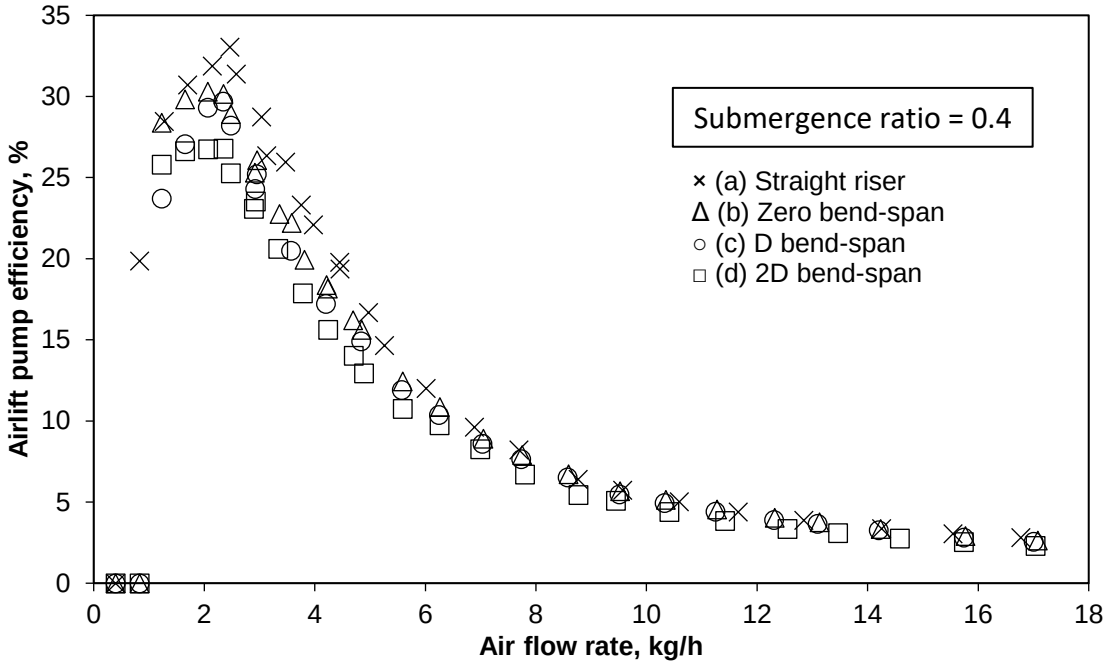

Fig. 7 Variation of airlift pump efficiency with air mass flow rate for different bend-span lengths

- L is the total riser length (m),
- Hs is the water level in the supply tank (m),
- Pin and Pan are the injection and atmospheric pressures (Pa), respectively.

Although mass flow rate and superficial velocity are standard parameters for characterising airlift performance, dimensionless analyses—such as those involving the Reynolds and Froude numbers—are often employed to enable broader applicability and scaling (Holagh & Ahmed, 2024).

As shown in Fig. 6, the water throughput pattern for all configurations is consistent with earlier observations by Fujimoto et al. (2005) and Yoshinaga and Sato (1996). The output begins at a minimum air flow rate required to initiate lifting, increases rapidly to a peak, slightly decreases, and then levels off at a higher steady value. Maximum throughput, reaching 554 kg/h, occurred within the churn flow regime, while the highest efficiency (33%) was achieved during slug flow conditions (Doucette et al., 2024).

Notably, introducing a bend into the riser reduces both peak and stable water delivery rates, with larger span lengths exacerbating this decline. In particular, the 2D configuration exhibited a drop of approximately 17% in peak and 15% in steady throughput compared to the straight pipe. These losses can be attributed to increased friction in the horizontal segment and added vortical resistance from eddies generated at the bends.

Despite the performance drop, all bent configurations shared the same cutoff air mass flow rate as the straight riser. As depicted in Figure 7, the bends caused a reduction in maximum pump efficiency—up to 6%—falling from 33% in the straight pipe to 26.7% in the longest span configuration. However, beyond an air mass flow rate of 6 kg/h, efficiency values converged across all configurations. This convergence is attributed to the higher injection pressure required to overcome additional friction and turbulence losses introduced by the bent geometry.

Figures 8 through 10 capture the flow behaviour observed in the three bent riser configurations under a relatively low air mass flow rate of 2 kg/h. In all cases, a repeating pattern characteristic of the slug–churn regime is evident. The sequence begins with gas bubbles gradually collecting along the upper surface of the horizontal segment (labelled as scene A). This is followed by the arrival of a large slug bubble (scene B), which displaces and sweeps the previously accumulated bubbles through the bend (scene C). As the slug exits into the downstream vertical section, a thin film of liquid is seen to flow backward along the lower wall of the horizontal segment (scene D), completing the cycle.

At a high air mass flow rate of 17 kg/h, the flow dynamics in the bent risers—illustrated in Figs. 11, 12, and 13—reveal a distinct phenomenon linked to fluid inertia. The water stream tends to detach from the left wall of the downstream vertical segment, forming a low-pressure separation region. Within this zone, air bubbles accumulate and coalesce into an air pocket. Over time, this pocket grows until it reaches a size at which the drag force exerted by the moving water is sufficient to displace it downstream. This behaviour is particularly pronounced in the riser with a 2D span, as shown in Fig. 13, and contributes to the observed degradation in pump performance for geometries with extended horizontal sections.

The intensified separation observed in the 2D configuration can be explained by analysing the velocity profile evolution, depicted schematically in Fig. 14. As the gas-liquid mixture moves through the first bend, centrifugal

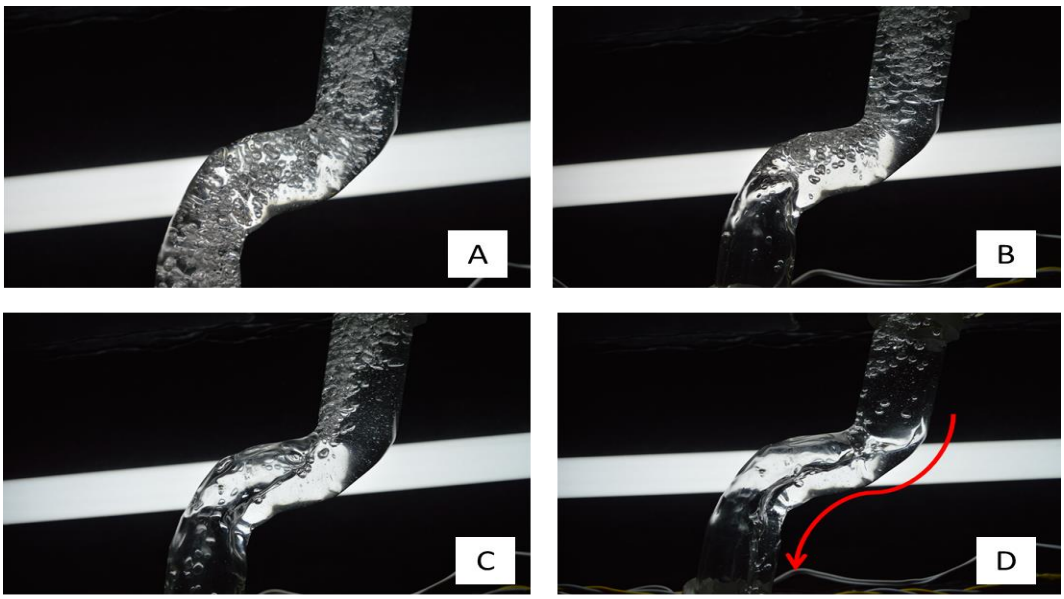

Fig. 8 Flow visualization of the Zero bend-span configuration at low air flow rate of 2 kg/h

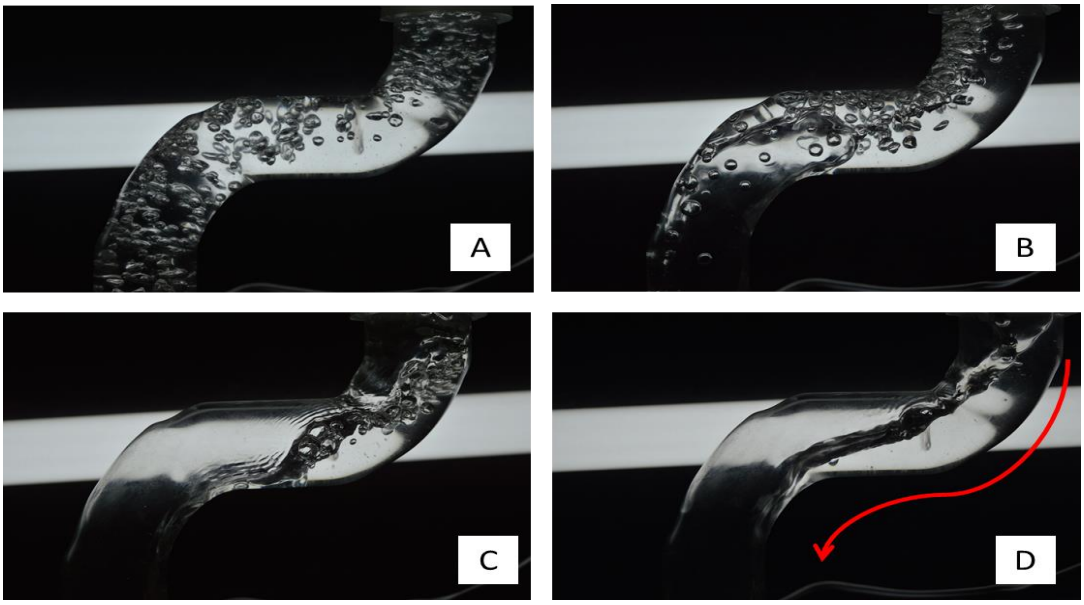

Fig. 9 Flow visualization of the D bend-span configuration at low air flow rate of 2 kg/h

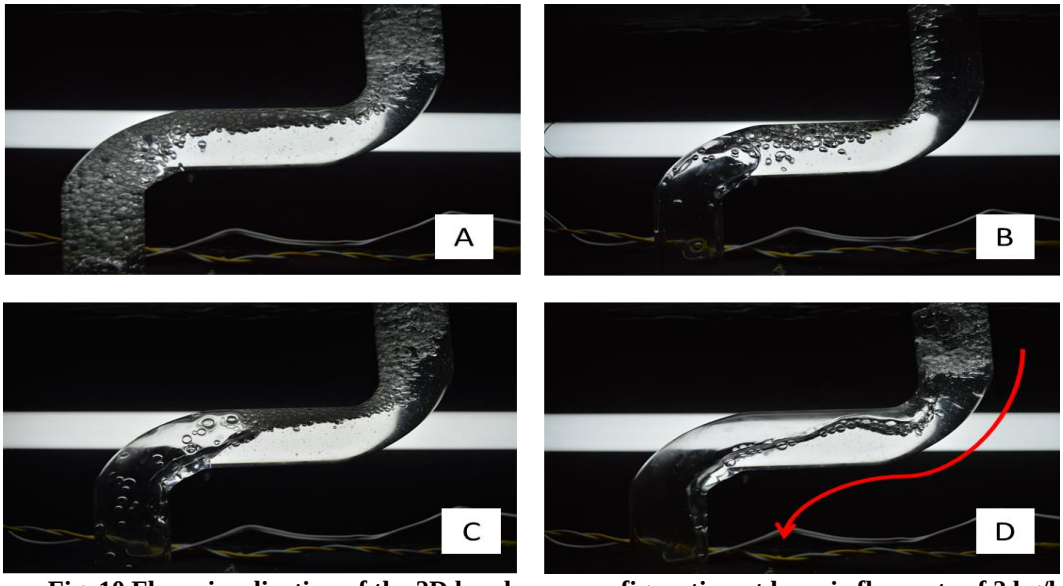

Fig. 10 Flow visualization of the 2D bend-span configuration at low air flow rate of 2 kg/h

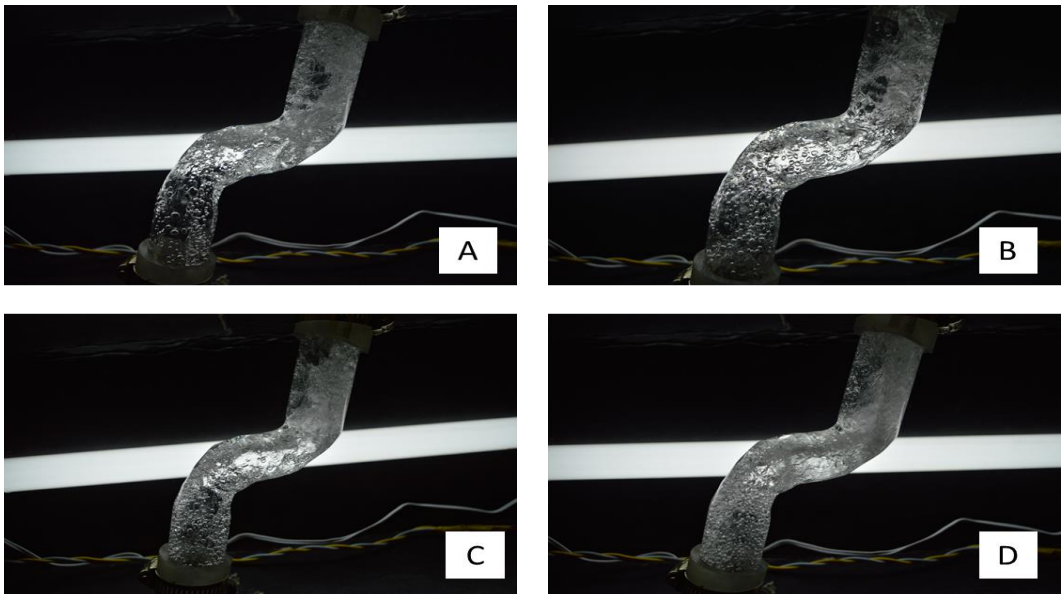

Fig. 11 Flow visualization of the Zero bend-span configuration at high air flow rate of 17 kg/h

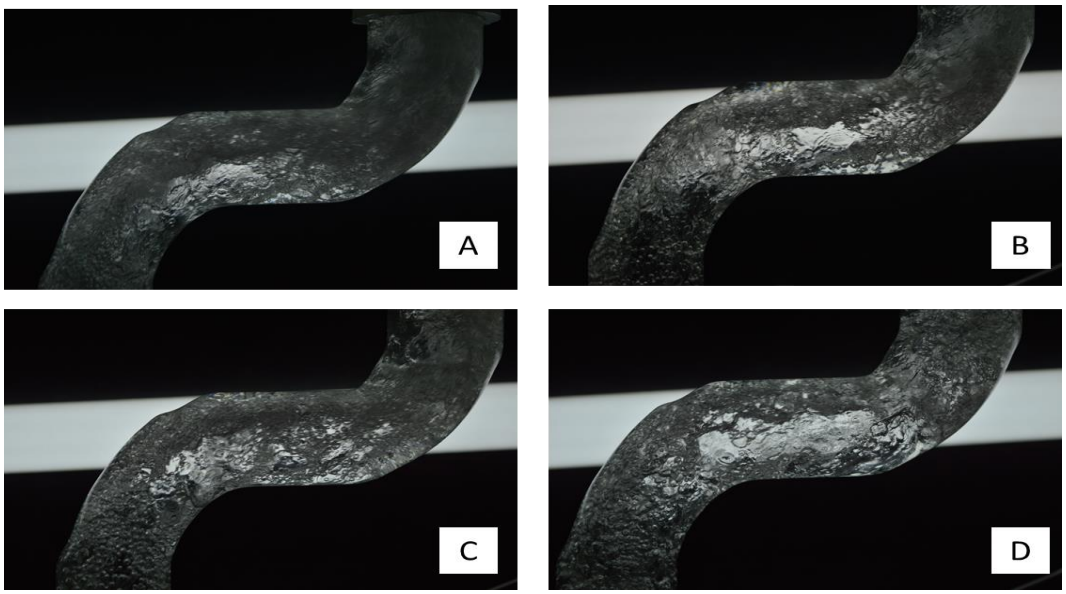

Fig. 12 Flow visualization of the D bend-span configuration at high air flow rate of 17 kg/h

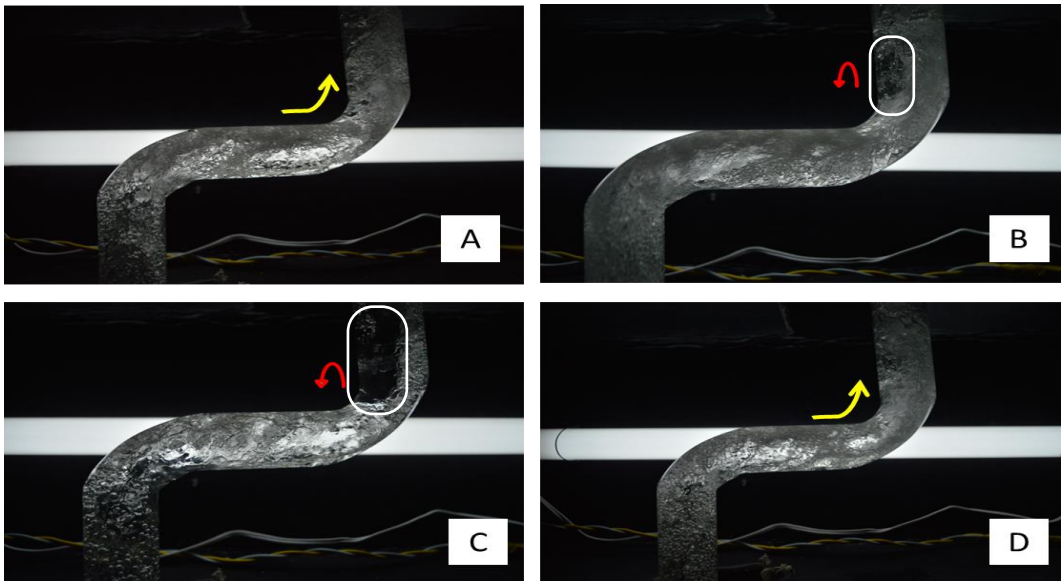

Fig. 13 Flow visualization of the 2D bend-span configuration at high air flow rate of 17 kg/h

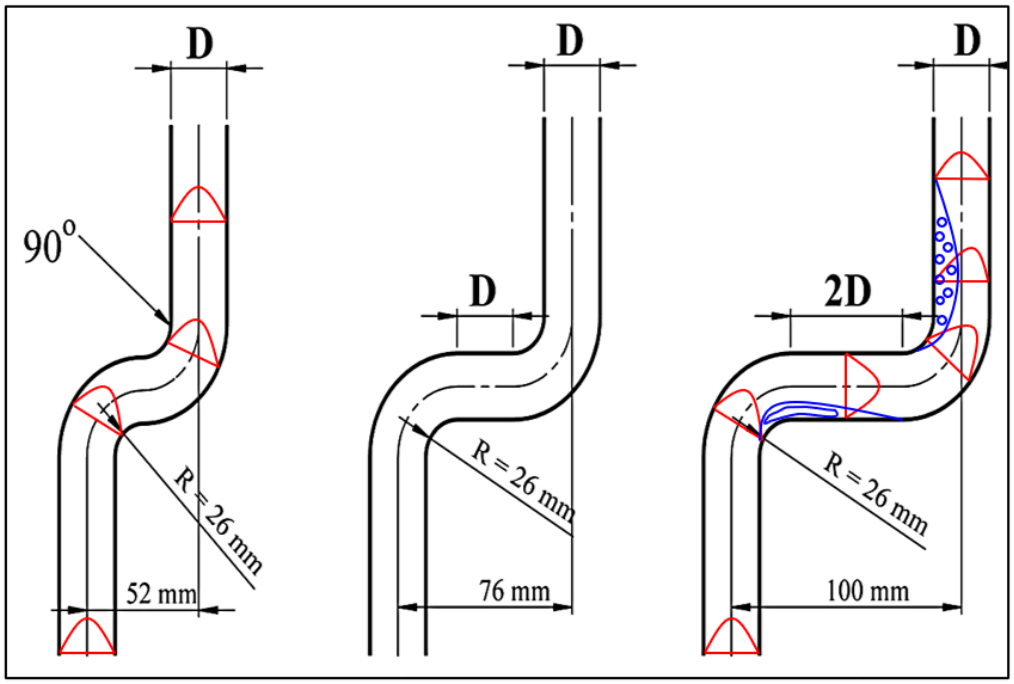

Fig. 14 Anticipated velocity profile evolution in the studied bend-spans

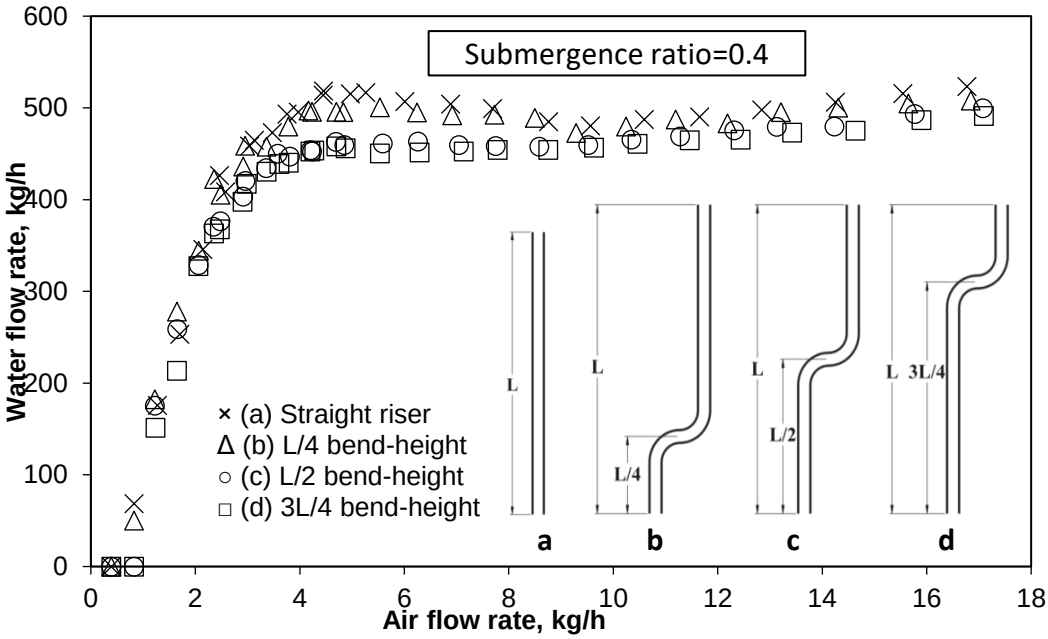

Fig. 15 Variation of water productivity with air mass flow rate for the tested bend-heights

forces cause the velocity profile to shift toward the left-hand wall. This asymmetry gradually dissipates in the horizontal section, restoring a more uniform distribution. However, as the flow encounters the second bend, the profile shifts again—this time toward the right wall—leading to detachment from the left wall and formation of a separation region.

In contrast, for the configurations with shorter bend spans (Zero and D), the intermediate horizontal section is insufficiently long for the flow to re-symmetrise. Consequently, the second bend is approached with a higher velocity near the left wall, which prevents separation and stabilises the flow. It is also important to note the presence of a secondary separation region at the exit of the first bend along the right wall. Nevertheless, in this location, any entrapped air bubbles are quickly released by buoyancy, preventing the formation of a stable air pocket.

3.2 Effect of Bend Position

To investigate how the vertical placement of a bend affects pump behaviour, the zero-span bend configuration was installed at three different heights along the riser: 1 m (L/4), 2 m (L/2), and 3 m (3L/4). Figures 15 and 16 display the corresponding variations in water output and pumping efficiency as the air mass flow rate changes.

As noted in previous findings by Kassab et al. (2023), the upper portion of the riser plays a critical role in determining

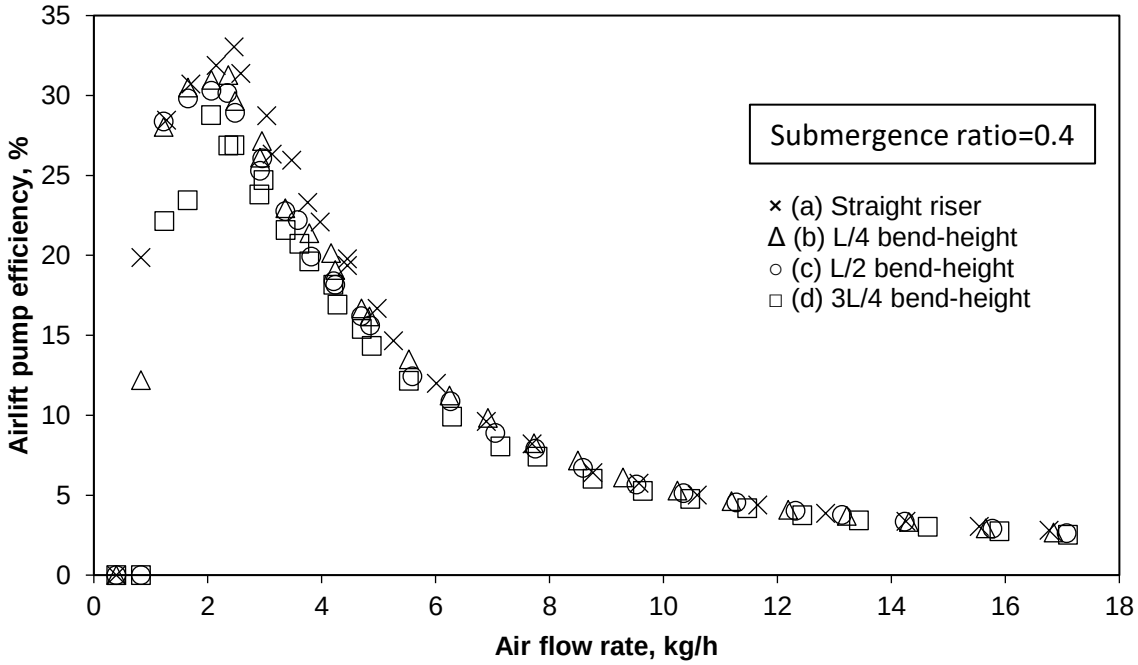

Fig. 16 Variation of airlift pump efficiency with air mass flow rate for the tested bend-heights

the system's throughput. This section carries the highest flow velocity and is thus subjected to increased frictional resistance, which in turn affects overall performance. This trend holds true in bent riser configurations as well—raising the location of the bend leads to a gradual decline in pump productivity. Specifically, water flow rate decreases by roughly 2% for each upward shift in the bend's elevation.

Efficiency trends in Figure 16 further support this observation. The straight riser delivers a peak efficiency of 33%, while the introduction of bends at L/4, L/2, and 3L/4 reduces this figure to 31.4%, 30.3%, and 28.8%, respectively.

Another notable effect occurs when the bent section is positioned at or above the submergence level. In these cases, the horizontal segment acts as a separation zone, where gravity facilitates the stratification of phases—air tends to rise while water descends. This phase separation delays the onset of net water delivery, increasing the required air mass flow rate from 0.4 to 0.8 kg/h for the L/2 and 3L/4 configurations.

3.3 Limitations of the Study

While the present study offers foundational insights into flow regime transitions and pump performance in vertical and bent airlift systems, extrapolating these results directly to oilfield conditions should be done with care. The current experiments use an air–water system, which is a common and safe proxy in two-phase flow research due to its reproducibility and relevance to fundamental flow dynamics.

However, realistic production fluids such as crude oil, natural gas, emulsions, and mixtures containing sand exhibit very different properties—particularly in terms of liquid viscosity. As reported by Fadlalla et al. (2023), higher viscosity leads to several changes: reduced pumping efficiency, earlier onset of flow regime transitions, higher void fractions, and the formation of larger Taylor bubbles. Therefore, the extension of these findings to actual field scenarios must account for such differences, and future work should focus on investigating airlift behaviour in more complex multiphase systems to enhance applicability.

4. CONCLUSIONS

This research highlights the detrimental impact of geometric irregularities—specifically bends—on the performance of airlift pumps. Both water delivery rate and energy efficiency are adversely affected when the riser deviates from a straight vertical configuration. The primary causes of performance decline are increased frictional and vortical resistance, which scale with the horizontal distance between bends, and flow separation phenomena that occur when bends are positioned above the submergence depth, leading to disrupted phase interaction.

Key observations from the study include:

- Introducing a horizontal bend with a span equal to twice the riser diameter results in a 15% decrease in water throughput, while relocating the bend to three-quarters of the riser height leads to a 6% reduction.
- When bends are placed above the submergence level, the air mass flow rate required to initiate lifting increases, posing a design challenge in systems where gas availability or pressure is constrained.
- Unique flow instabilities such as cyclic slug-churn dynamics at low air injection rates and air pocket formation at high rates were observed in

the bent sections. These patterns are exclusive to non-vertical layouts and signify additional sources of energy loss.

The insights gained from this investigation offer practical guidance for the design and operation of directional airlift systems, especially in applications such as oil and gas extraction. Careful attention to bend positioning and spacing is essential to minimise efficiency losses and maintain stable two-phase flow.

CONFLICT OF INTEREST

The authors declare that they have no known competing financial interests or personal relationships that could have appeared to influence the work reported in this manuscript.

AUTHORS CONTRIBUTION

Sadek Z. Kassab: Conceptualisation – Methodology – Writing – Review & Editing – Supervision. **Abdel-Rahman Amr Abdel-Razek:** Methodology – Validation – Formal Analysis – Data Curation – Writing – Original Draft – Visualisation. **Eslam R. Lotfy:** Formal Analysis – Investigation – Data Curation – Writing – Original Draft

REFERENCES

Arabjamaloei, R., Edalatkhah, S., & Jamshidi, E. (2011). A new approach to well trajectory optimization based on rate of penetration and wellbore stability. *Petroleum Science and Technology*, *29*(6), 588–600. https://doi.org/10.1080/10916460903419172

Bukhari, S. S., Abed, R., Holagh, S. G., & Ahmed, W. H. (2024). Flow pattern dependent model for airlift pumps performance: Analytical simulation and experimental verification. *Chemical Engineering Research and Design*, *201*, 67–81. https://doi.org/10.1016/J.CHERD.2023.11.033

Cho, N. C., Hwang, I. J., Lee, C. M., & Park, J. W. (2009). An experimental study on the airlift pump with air jet nozzle and booster pump. *Journal of Environmental Sciences*, *21*, S19–S23. https://doi.org/10.1016/S1001-0742(09)60028-0

Doucette, A., Holagh, S. G., & Ahmed, W. H. (2024). Experimental evaluation of airlift pumps' thermal and mass transfer capabilities. *Experimental Thermal and Fluid Science*, *154*, 111174. https://doi.org/10.1016/J.EXPTHERMFLUSCI.2024.111174

Elbanna, A. M. (2016). *A simple control model for the mud pump in drilling fluid systems of directional Drilling*. Alexandria University.

Enany, P., & Drebenshtedt, C. (2024). Performance characteristics of the airlift pump under vertical solid–water–gas flow conditions for conveying centimetric-sized coal particles. *International Journal of Coal Science and Technology*, *11*(1), 1–14. https://doi.org/10.1007/S40789-024-00668-Y/FIGURES/7

Fadlalla, D., Rosettani, J., Holagh, S. G., & Ahmed, W. H. (2023). Airlift pumps characteristics for shear-thinning non-Newtonian fluids: An experimental investigation on liquid viscosity impact. *Experimental Thermal and Fluid Science*, *149*, 110994. https://doi.org/10.1016/J.EXPTHERMFLUSCI.2023.110994

Fan, W., Chen, J., Pan, Y., Huang, H., Arthur Chen, C.-T., & Chen, Y. (2013). Experimental study on the performance of an air-lift pump for artificial upwelling. *Ocean Engineering*, *59*, 47–57. https://doi.org/10.1016/j.oceaneng.2012.11.014

Fan, W., Zhang, Z., Yao, Z., Xiao, C., Zhang, Y., Zhang, Y., Liu, J., Di, Y., Chen, Y., & Pan, Y. (2020). A sea trial of enhancing carbon removal from Chinese coastal waters by stimulating seaweed cultivation through artificial upwelling. *Applied Ocean Research*, *101*, 102260. https://doi.org/10.1016/j.apor.2020.102260

Fujimoto, H., Murakami, S., Omura, A., & Takuda, H. (2004). Effect of local pipe bends on pump performance of a small air-lift system in transporting solid particles. *International Journal of Heat and Fluid Flow*, *25*(6), 996–1005. https://doi.org/10.1016/j.ijheatfluidflow.2004.02.025

Fujimoto, H., Nagatani, T., & Takuda, H. (2005). Performance characteristics of a gas–liquid–solid airlift pump. *International Journal of Multiphase Flow*, *31*(10–11), 1116–1133. https://doi.org/10.1016/j.ijmultiphaseflow.2005.06.008

Hanafizadeh, P., Saidi, M. H., Karimi, A., & Zamiri, A. (2010). Effect of bubble size and angle of tapering upriser pipe on the performance of airlift pumps. *Particulate Science and Technology*, *28*(4), 332–347. https://doi.org/10.1080/02726351.2010.496300

Holagh, S. G., & Ahmed, W. H. (2024). Critical review of vertical gas-liquid slug flow: An insight to better understand flow hydrodynamics' effect on heat and mass transfer characteristics. *International Journal of Heat and Mass Transfer*, *225*, 125422. https://doi.org/10.1016/J.IJHEATMASSTRANSFER.2024.125422

Hu, D., Tang, C. L., Cai, S. P., & Zhang, F. H. (2012). The Effect of air injection method on the airlift pump performance. *Journal of Fluids Engineering*, *134*(11). https://doi.org/10.1115/1.4007592

Kassab, S. Z., Abdelrazek, A. A., & Lotfy, E. R. (2022). Effects of injection mechanism on air-water air lift pump performance. *Alexandria Engineering Journal*, *61*(10), 7541–7553. https://doi.org/10.1016/j.aej.2022.01.002

Kassab, S. Z., Abdelrazek, A. A., & Lotfy, E. R. (2023). Effect of the up-riser pipe diameter discontinuity on the airlift pump performance. *Experimental Thermal*

and Fluid Science, *149*, 111028. https://doi.org/10.1016/j.expthermflusci.2023.111028

Kassab, S. Z., Kandil, H. A., Warda, H. A., & Ahmed, W. H. (2009). Air-lift pumps characteristics under two-phase flow conditions. *International Journal of Heat and Fluid Flow*, *30*(1), 88–98. https://doi.org/10.1016/j.ijheatfluidflow.2008.09.002

Kim, S. H., Sohn, C. H., & Hwang, J. Y. (2014). Effects of tube diameter and submergence ratio on bubble pattern and performance of air-lift pump. *International Journal of Multiphase Flow*, *58*, 195–204. https://doi.org/10.1016/J.IJMULTIPHASEFLOW.2013.09.007

Kumar, D., Amudha, K., Gopakumar, K., & Ramadass, G. A. (2024). Air-lift pump systems for vertical solid particle transport: A comprehensive review and deep sea mining potential. *Ocean Engineering*, *297*, 116928. https://doi.org/10.1016/J.OCEANENG.2024.116928

Nicklin, D. (1963). The air-lift pump: theory and optimisation. *Transactions of the Institution of Chemical Engineers*, *41*, 29–39.

Okon, E. I., & Ndubuka, C. I. (2023). Analysis of crude oil production with gas lift methods. *Petroleum Science and Technology*, 1–30. https://doi.org/10.1080/10916466.2023.2174554

Qiang, Y., Fan, W., Xiao, C., Pan, Y., & Chen, Y. (2018). Effects of operating parameters and injection method on the performance of an artificial upwelling by using airlift pump. *Applied Ocean Research*, *78*, 212–222. https://doi.org/10.1016/j.apor.2018.06.006

Samaras, V. C., & Margaris, D. P. (2005). Two-phase flow regime maps for air-lift pump vertical upward gas–liquid flow. *International Journal of Multiphase Flow*, *31*(6), 757–766. https://doi.org/10.1016/j.ijmultiphaseflow.2005.03.001

Shallouf, M., Ahmed, W., & Abdou, S. (2019, June). *Numerical Analysis of Fluid Flow in Aquaculture Systems*. https://doi.org/10.11159/ffhmt19.179

Tighzert, H., Brahimi, M., Kechroud, N., & Benabbas, F. (2013). Effect of submergence ratio on the liquid phase velocity, efficiency and void fraction in an air-lift pump. *Journal of Petroleum Science and Engineering*, *110*, 155–161. https://doi.org/10.1016/J.PETROL.2013.08.047

Yoshinaga, T., & Sato, Y. (1996). Performance of an air-lift pump for conveying coarse particles. *International Journal of Multiphase Flow*, *22*(2), 223–238. https://doi.org/10.1016/0301-9322(95)00067-4